

Groundwater

Hydraulic-Head Formulation for Density-Dependent Flow and Transport

by Christian D. Langevin¹, Sorab Panday^{2,3}, and Alden M. Provost⁴

Abstract

Density-dependent flow and transport solutions for coastal saltwater intrusion investigations, analyses of fluid injection into deep brines, and studies of convective fingering^{3,1} and instabilities of denser fluids moving through less dense fluids typically formulate the groundwater flow equation in terms of pressure or equivalent freshwater head. A formulation of the flow equation in terms of hydraulic head is presented here as an alternative. The hydraulic-head formulation can facilitate adaptation of existing constant-density groundwater flow codes to include density-driven flow by avoiding the need to convert between freshwater head and hydraulic head within the code and by incorporating density-dependent terms as a compartmentalized "correction" to constant-density calculations already performed by the code. The hydraulic-head formulation also accommodates complexities such as unconfined groundwater flow and Newton-Raphson solution schemes more readily than the freshwater-head formulation. Simulation results are presented for four example problems solved using an implementation of the hydraulic-head formulation in MODFLOW.

Introduction

Saltwater intrusion modeling codes such as SEAWAT (Guo and Langevin 2002; Langevin et al. 2003, 2008) formulate the density-dependent groundwater flow equation in terms of equivalent freshwater head (called simply freshwater head throughout the remainder of this paper). The freshwater-head formulation is easy to conceptualize, and the resulting generalized form of Darcy's Law, which relates specific discharge to the forces that drive flow, can be written as the sum of a freshwater-head term and a density-dependent term. The freshwater-head gradient is the sole driving force for horizontal flow; for vertical flow, the density-dependent term also contributes to the flux calculation. Once the freshwater-head formulation is solved for flow, the resulting fluxes are incorporated into a solute-transport model that solves for the distribution of solute concentration. However, the concentration distribution affects the fluid-density distribution, which in

turn affects the groundwater flow field. Thus, the solution progresses in an iterative or time-lagged fashion, alternately updating and solving the variable-density flow equation and the solute-transport equation.

Although the freshwater-head formulation is conceptually appealing and convenient for calculating groundwater fluxes, some calculations in a groundwater model are best (or necessarily) performed using other types of head, such as hydraulic head. Thus, use of the freshwater-head formulation typically requires repeated conversion between freshwater head and another type of head within the modeling code. In modeling codes such as SEAWAT, hydraulic heads correspond to water-table elevations in unconfined model cells. Therefore, hydraulic heads (not freshwater heads) determine whether cells are confined, unconfined, or dry, or whether dry cells should rewet, and transmissivities computed in unconfined cells depend on hydraulic head. In codes that simulate variably saturated flow, moisture retention curves are expressed as functions of pressure head (hydraulic head minus elevation), not freshwater head. Also, in codes based on the freshwater-head formulation, prescribed-head and head-dependent boundary conditions ultimately need to be represented in terms of freshwater head. Therefore, either the user must calculate and specify approximate freshwater-head boundary values a priori in the model input, or a conversion from user-specified hydraulic-head values to freshwater heads must be performed within the code on every solution iteration to account for changes in density, which can destabilize the solution. Moreover, use of the freshwater-head formulation can render other

¹Corresponding author: Integrated Modeling and Prediction Division, U.S. Geological Survey, MN 55112; langevin@usgs.gov

²GSI Environmental Inc., 626 Grant St., Ste. C, Herndon, VA, 20170

³Department of Biological Systems Engineering University of Nebraska-Lincoln 223 L. W. Chase Hall, East Campus P. O. Box 830726 Lincoln, NE, 68583-0726

⁴Integrated Modeling and Prediction Division U.S. Geological Survey, Reston, VA.

Received September 2019, accepted November 2019.

Published 2019. This article is a U.S. Government work and is in the public domain in the USA.

doi: 10.1111/gwat.12967

calculations more complex. For example, if the Newton-Raphson method is used to resolve nonlinearities in the governing equations, the Jacobian derivative terms need to be expanded in terms of freshwater head. Also, expanding the freshwater head to turbulent or viscous flow equations (Shoemaker et al. 2008) and treatment of associated nonlinearities may not be straightforward.

This paper describes a formulation of the density-dependent groundwater flow equation in terms of hydraulic head. The hydraulic-head formulation is attractive for several reasons. First, hydrologists typically conceptualize groundwater flow in terms of hydraulic head. Second, in the hydraulic-head formulation, the generalized form of Darcy's Law can be written as the sum of the familiar, constant-density, hydraulic-head term, and additional, density-dependent terms. Thus, the impact of the density-dependent terms can be grasped intuitively as a modification of constant-density behavior. An additional benefit of this decomposition of terms is that the density-dependent terms can be readily incorporated as a "density correction" into constant-density groundwater codes that are based on hydraulic head, with the density-dependent calculations compartmentalized to minimize disruption of the existing code. Third, expressing all calculations in terms of hydraulic head precludes the need to convert between freshwater head and hydraulic head and avoids complexities associated with boundary conditions and nonlinearities. Finally, the methodology described here can be readily adapted to turbulent-flow or viscous-flow equations, as well.

The hydraulic-head-based approach described in this paper is similar to the approach implemented in MOC-DENS3D (Oude Essink 1998) in that it is based on the assumption that fluid density does not vary with concentration and/or temperature except where it appears in the density-dependent version of Darcy's Law. As a result, the approach described here, like the approach in MOC-DENS3D, is founded on the same "conservation-of-volume" equation that is the basis for most constant-density groundwater modeling codes. A crucial difference, however, is that whereas MOC-DENS3D is formulated in terms of freshwater head, the approach described here is formulated entirely in terms of hydraulic head, thereby offering the benefits discussed earlier.

The hydraulic-head formulation for density-dependent flow has been implemented within the conceptual framework used in the MODFLOW family of codes (McDonald and Harbaugh 1988; Harbaugh et al. 2000; Harbaugh 2005; Niswonger et al. 2011; Langevin et al. 2017), and the discussion in this paper is framed primarily in terms of MODFLOW. However, the approach applies generally to any numerical groundwater flow model based on hydraulic head and can be readily implemented in other subsurface flow and transport models, such as Hydrus (Simunek et al. 1998), MODFLOW/MT3DMS (Zheng and Wang 1999), and MIKE SHE (Danish Hydrologic Institute 1998), for example. The method is also applicable to surface water flow or

pipe flow interacting with groundwater flow and can be extended to non-Darcy flow conditions.

The remainder of this paper begins with the derivation of a density-dependent form of Darcy's Law in terms of hydraulic head. Then, corresponding expressions for flows between cells and at head-dependent boundaries in a control-volume finite-difference model are derived, and ways to incorporate the resulting density-dependent terms into the numerical representation of the flow equation are proposed. The paper concludes with four example problems that demonstrate the implementation and accuracy of the hydraulic-head formulation.

Formulation and Implementation

Density-dependent groundwater flow is described mathematically by a conservation-of-mass equation together with a density-dependent form of Darcy's Law. The new hydraulic-head formulation for density-dependent flow is based on the simplifying assumption that fluid density is constant in all terms of the governing equations except the storage term in the conservation-of-mass equation, in which density varies implicitly with pressure, and in Darcy's Law, in which density is allowed to vary as a function of concentration or temperature. As a result, the hydraulic-head formulation uses the same approximate conservation equation that is solved in most constant-density groundwater models, including MODFLOW (Langevin et al. 2017):

$$S_S \frac{\partial h}{\partial t} = -\nabla \cdot \mathbf{q} + Q_s, \quad (1)$$

where S_S is a storage coefficient, called specific storage, that describes the volume of water released from storage per unit volume per unit change in hydraulic head, h is the hydraulic head, t is time, \mathbf{q} is the vector of specific discharge, $\nabla \cdot \mathbf{q}$ is the divergence of \mathbf{q} , and Q_s is the sum of external sources and sinks of fluid volume. The left-hand side represents the volumetric rate (volume of water per time, per volume of aquifer) at which water goes into or comes out of compressive storage due to changes in hydraulic head, and the right-hand side represents the net volumetric rate of inflow of water per volume of aquifer. Therefore, Equation 1 represents a "conservation of volume" at each point in the aquifer.

The control-volume finite-difference approach used in MODFLOW results in a discrete conservation-of-volume equation for each cell of the form

$$\sum_{m=1}^{M_n} Q_{nm} + Q_{ns} - S_{Sn} V_n \frac{\Delta h_n}{\Delta t} = 0, \quad (2)$$

where subscript n denotes the model cell over which the water balance is written, subscript m denotes cells that are neighbors of cell n , M_n is the number of neighbors of cell n , the summation is over all neighbors of cell n , Q_{nm} is the volumetric flow rate between cell n and cell m designated as positive for flow from cell m into cell n , Q_{ns}

is the sum of external sources and sinks acting on cell n , S_{Sn} is the specific storage for cell n , V_n is the volume of cell n , h_n is the hydraulic head in cell n , and Δ represents a change in a quantity during the current simulation time step. The first, second, and third terms in Equation 2 are discrete analogs of the divergence, external source/sink, and storage terms in Equation 1, respectively.

Each of the three terms in Equation 2 can, in general, depend on the hydraulic-head values in cell n and its neighbors m . On each simulation time step, the goal of the solution algorithm is to calculate head values in each cell that are consistent with the set of conservation-of-volume equations (Equation 2) for all model cells. In MODFLOW, as in many groundwater flow simulators, the set of cellwise conservation-of-volume equations for a model with N cells is expressed as a linear system of equations of the form

$$\mathbf{Ah} = \mathbf{b}, \quad (3)$$

where \mathbf{A} is an $N \times N$ coefficient matrix, \mathbf{h} is a vector of N cellwise values of the dependent variable (head), and \mathbf{b} is a right-hand-side vector of length N . After Equation 2 is expanded in terms of cellwise head values, coefficients that multiply head values being solved for on the current time step are incorporated into the coefficient matrix, \mathbf{A} , and all other terms are moved to the right-hand side and incorporated into vector \mathbf{b} . For many problems, the coefficients in the \mathbf{A} matrix depend on head. For example, in unconfined groundwater flow, transmissivities are head dependent, leading to head-dependent coefficients in \mathbf{A} . In such problems, which are inherently nonlinear, \mathbf{A} is reformulated using the latest calculated head values and the system of equations is resolved repeatedly until convergence of the solution is achieved. Head-based variable-density codes, such as SEAWAT (Langevin et al. 2008), often formulate their nonlinear water-conservation equations as linear systems and solve them iteratively, as well. In such codes, the dependent variable is typically freshwater head, but in the formulation presented in this paper, the dependent variable is hydraulic head.

The remainder of this section focuses on a hydraulic-head formulation for flow between cells, Q_{nm} , in Equation 2. A form of Darcy's Law that relates specific discharge to hydraulic head is derived and discretized to obtain a density-dependent expression for Q_{nm} (and an analogous expression for head-dependent boundary conditions), and ways to incorporate the density-dependent terms into the linear system (Equation 3) are proposed.

Specific Discharge in Terms of Hydraulic Head

When the fluid density varies spatially, the specific discharge vector, \mathbf{q} (which comprises the components of the volumetric groundwater flux in each of the coordinate directions, x , y , and z), is commonly expressed in terms of pressure, P (de Marsily 1986, 63):

$$\mathbf{q} = -\frac{\mathbf{k}}{\mu}(\nabla P + \rho g \nabla z), \quad (4)$$

where \mathbf{k} is the intrinsic permeability tensor, μ is dynamic viscosity, ρ is fluid density, g is the magnitude of gravitational acceleration, z is elevation, and ∇ is the gradient operator. Hydraulic head, h , defined as

$$h = z + \frac{P}{\rho g}, \quad (5)$$

is the height to which water having the same density as the groundwater would rise in a tightly cased well open to a single point in the aquifer. For an isotropic porous medium, that is, for a porous medium in which the effective hydraulic conductivity is the same regardless of flow direction, the tensor \mathbf{k} is replaced by a scalar intrinsic permeability, k , and Equation 5 can be solved for pressure and substituted into Equation 4, which can then be manipulated to give

$$\mathbf{q} = -\frac{\mu_0 k \rho_0 g}{\mu} \left[\nabla \left(\frac{\rho}{\rho_0} h \right) - z \nabla \frac{\rho}{\rho_0} \right], \quad (6)$$

where ρ_0 and μ_0 are, respectively, the density and dynamic viscosity of a reference fluid (typically freshwater). Use of the chain rule, grouping of terms, and approximation of the ratio $\frac{\mu_0}{\mu}$ as one allows Equation 6 to be rewritten as

$$\mathbf{q} = -K_0 \left[\frac{\rho}{\rho_0} \nabla h + (h - z) \nabla \frac{\rho}{\rho_0} \right], \quad (7)$$

where $K_0 = \frac{k \rho_0 g}{\mu_0}$ is the hydraulic conductivity for aquifer material saturated with reference fluid. This mathematical form of the specific discharge equation (Equation 7) is desirable, because it contains a gradient of head term, which is what is used as the driving force in most constant-density groundwater flow simulators. Equation 7 can also be written in the form

$$\mathbf{q} = -K_0 \left[\nabla h + \left(\frac{\rho}{\rho_0} - 1 \right) \nabla h + (h - z) \nabla \frac{\rho}{\rho_0} \right], \quad (8)$$

to facilitate comparison with the constant-density equation for specific discharge,

$$\mathbf{q} = -K \nabla h, \quad (9)$$

and the variable-density, freshwater-head equation for specific discharge,

$$\mathbf{q} = -K_0 \left[\nabla h_0 + \left(\frac{\rho}{\rho_0} - 1 \right) \nabla z \right], \quad (10)$$

where h_0 is freshwater head, that is, the height to which water having the density of freshwater would rise in a tightly cased well open to a single point in the aquifer.

Density-Dependent Flow Between Cells

The density-dependent terms of the hydraulic-head formulation can be incorporated into an existing constant-density modeling code by updating the flow calculation

between any two cells to use a form of Equation 8. For a control-volume finite-difference program like MODFLOW, the discretized form of Equation 8 that represents the flow between a pair of neighboring cells (Q_{nm} in Equation 2) is

$$Q_{nm} = q_{nm} A_{nm} \\ = \frac{K_0 A_{nm}}{L_{nm} + L_{mn}} \left[(h_m - h_n) + \left(\frac{\rho_{nm}}{\rho_0} - 1 \right) (h_m - h_n) \right. \\ \left. + (h_{nm} - z_{nm}) \frac{\rho_m - \rho_n}{\rho_0} \right], \quad (11)$$

where q_{nm} is the specific discharge between cells n and m , A_{nm} is the area of flow between cells n and m , L_{nm} is the distance from the center of cell n to its shared face with cell m , and L_{mn} is the distance from the center of cell m to its shared face with cell n . The subscripts in Equation 11 indicate the locations where the variables are evaluated. Variables h_{nm} , z_{nm} , and ρ_{nm} are, respectively, the head, elevation, and density interpolated between the centers of cells n and m , at the shared interface between the two cells:

$$h_{nm} = (1 - \omega)h_n + \omega h_m \\ z_{nm} = (1 - \omega)z_n + \omega z_m \\ \rho_{nm} = \omega \rho_n + (1 - \omega) \rho_m, \quad (12)$$

where

$$\omega = \frac{L_{nm}}{L_{nm} + L_{mn}} \quad (13)$$

is a weighting factor based on the distances between the cell centers and the shared face.

Equation 11 can be decomposed into the form

$$Q_{nm} = Q_{nm}^{CD} + \Delta Q_{nm}^{HH}, \quad (14)$$

where

$$Q_{nm}^{CD} = C_{nm}(h_m - h_n), \quad (15)$$

$$\Delta Q_{nm}^{HH} = C_{nm} \left[\left(\frac{\rho_{nm}}{\rho_0} - 1 \right) (h_m - h_n) \right. \\ \left. + (h_{nm} - z_{nm}) \frac{\rho_m - \rho_n}{\rho_0} \right], \quad (16)$$

and

$$C_{nm} = \frac{K_0 A_{nm}}{L_{nm} + L_{mn}} \quad (17)$$

is a hydraulic conductance between cells n and m . Equation 15 is the conductance-based formulation used by the MODFLOW family of codes to compute constant-density flow between cells, and Equation 16 represents

additional terms associated with the hydraulic-head formulation for density-dependent flow. Thus, the total flow in the hydraulic-head formulation (Equation 14) is expressed as the sum of the constant-density flow, Q_{nm}^{CD} , and a density-dependent correction, ΔQ_{nm}^{HH} . The advantage of decomposing the flow expression in this way is that the effects of density variations can be incorporated into any model that already computes Q_{nm}^{CD} simply by adding ΔQ_{nm}^{HH} , and density calculations can be compartmentalized and put into a separate module.

Addition of Density-Dependent Terms to the Linear System of Equations

Depending on how it is incorporated into the linear system of equations (Equation 3), the density-dependent correction ΔQ_{nm}^{HH} (Equation 16) can modify the coefficient matrix, \mathbf{A} , and/or the right-hand-side vector, \mathbf{b} . One option is to take h_n and h_m in Equation 16 to be head values for the current time step, which are the values being solved for, and to use values from the previous time step for the remaining variables. In that case, the coefficients associated with h_n and h_m modify, respectively, diagonal (n, n) and off-diagonal (n, m) entries in row n of the coefficient matrix, and the remaining term modifies the right-hand-side vector:

$$A_{n,n} \leftarrow A_{n,n} - C_{nm} \left(\frac{\rho_{nm}}{\rho_0} - 1 \right) \\ A_{n,m} \leftarrow A_{n,m} + C_{nm} \left(\frac{\rho_{nm}}{\rho_0} - 1 \right) \quad (18)$$

and

$$b_n \leftarrow b_n - C_{nm}(h_{nm} - z_{nm}) \frac{\rho_m - \rho_n}{\rho_0}, \quad (19)$$

where $A_{n,m}$, for example, denotes the off-diagonal coefficient in row n and column m of matrix \mathbf{A} , and b_n denotes the n th entry in vector \mathbf{b} .

Alternatively, after substituting in the expression given in Equation 12 for the interpolated head, h_{nm} , into Equation 16, the latter equation can be rewritten as

$$\Delta Q_{nm}^{HH} = -C_{nm} \left[\left(\frac{\rho_{nm}}{\rho_0} - 1 \right) - (1 - \omega) \frac{\rho_m - \rho_n}{\rho_0} \right] h_n \\ + C_{nm} \left[\left(\frac{\rho_{nm}}{\rho_0} - 1 \right) + \omega \frac{\rho_m - \rho_n}{\rho_0} \right] h_m - C_{nm} z_{nm} \frac{\rho_m - \rho_n}{\rho_0}. \quad (20)$$

If h_n and h_m in Equation 20 are once again taken to be head values for the current time step and densities are evaluated on the previous timestep, the coefficient matrix is updated as

$$A_{n,n} \leftarrow A_{n,n} - C_{nm} \left[\left(\frac{\rho_{nm}}{\rho_0} - 1 \right) - (1 - \omega) \frac{\rho_m - \rho_n}{\rho_0} \right] \\ A_{n,m} \leftarrow A_{n,m} + C_{nm} \left[\left(\frac{\rho_{nm}}{\rho_0} - 1 \right) + \omega \frac{\rho_m - \rho_n}{\rho_0} \right] \quad (21)$$

and the right-hand-side vector is updated as

$$b_n \leftarrow b_n + C_{nm} z_{nm} \frac{\rho_m - \rho_n}{\rho_0}. \quad (22)$$

Testing with the hydraulic-head formulation thus far has shown that the implementation defined by Equations 21 and 22 is generally faster than the implementation defined by Equations 18 and 19.

Head-Dependent Boundary Conditions

Specified-flux boundaries do not require any special adjustment for the freshwater head and hydraulic-head formulations, so these parts of an existing code that implement specified-flux boundary conditions should not need to be modified. For specified-head boundaries, however, the dependence of hydraulic head on groundwater concentration, which could potentially change during the simulation, introduces additional considerations. In SEAWAT, head values input to the model and output from the model are hydraulic-head values, but the main internal calculations are performed in terms of freshwater heads. SEAWAT converts hydraulic heads input to the model, including initial and boundary heads, to freshwater heads, and once the internal calculations are completed, converts freshwater heads back to hydraulic heads for output. However, hydraulic head is defined in terms of the density of the groundwater at the point in the aquifer at which the head is calculated, and the conversion between hydraulic head and freshwater head depends on the density at that point. Even if the specified boundary head remains constant throughout the simulation, changes in concentration at the boundary can cause changes in density as the simulation progresses. As a result, the equivalent freshwater head at the specified-head boundary can change, causing the hydraulic behavior of the boundary to change. This is not a concern if the specified-head boundary is also a specified-concentration boundary, but in general, the concentration at a specified-head boundary may change with time, and the resulting changes in boundary behavior may not be desirable. Therefore, SEAWAT offers several options that allow the specified boundary head to be defined in terms of a reference density other than the calculated groundwater density at that boundary point, thereby allowing the boundary condition to better represent the desired behavior in a variety of hydraulic settings, as described in Langevin et al. (2008). In the hydraulic-head-based approach described in this paper, conversion between hydraulic head and freshwater head is not an issue. Nevertheless, changes in density at a specified-head boundary can change the physical ramifications of maintaining the specified hydraulic-head value, and reference-density options similar to those offered by SEAWAT could be applied to the hydraulic-head formulation to achieve better representation of the desired boundary behavior.

For a head-dependent boundary, such as the general head boundary in MODFLOW, the flow between cell n and a boundary l can be written for variable-density

conditions as

$$Q_{nl} = C_{nl} \left[(h_l - h_n) + \left(\frac{\rho_{nl}}{\rho_0} - 1 \right) (h_l - h_n) + (h_{nl} - z_{nl}) \frac{\rho_l - \rho_n}{\rho_0} \right], \quad (23)$$

where the l subscript indicates values associated with the boundary. Equation 23 is analogous to Equation 11, with the boundary head, h_l , replacing the head in cell m , h_m , and a boundary conductance, C_{nl} , replacing the intercell conductance defined in Equation 17, C_{nm} . Then, by analogy with Equation 16, the existing boundary flow calculations can be supplemented with a density correction term ΔQ_{nl}^{HH} , written as

$$\Delta Q_{nl}^{HH} = C_{nl} \left[\left(\frac{\rho_{nl}}{\rho_0} - 1 \right) (h_l - h_n) + (h_{nl} - z_{nl}) \frac{\rho_l - \rho_n}{\rho_0} \right]. \quad (24)$$

If h_{nl} is set to the arithmetic average of the head in cell n and the boundary head, $h_{nl} = (h_n + h_l)/2$, this density correction term can be added to the system of equations by updating the diagonal term of row n as

$$A_{n,n} \leftarrow A_{n,n} - C_{nl} \left[\left(\frac{\rho_{nl}}{\rho_0} - 1 \right) - \frac{1}{2} \frac{\rho_l - \rho_n}{\rho_0} \right], \quad (25)$$

and the right-hand-side vector as

$$b_n \leftarrow b_n - C_{nl} \left[\left(\frac{\rho_{nl}}{\rho_0} - 1 \right) h_l + \left(\frac{1}{2} h_l - z_{nl} \right) \frac{\rho_l - \rho_n}{\rho_0} \right]. \quad (26)$$

Alternative approaches for approximating h_{nl} could easily be implemented, but the arithmetic approach is advantageous in that no additional user input is required.

Examples

The hydraulic-head formulation was implemented in MODFLOW 6 (Hughes et al. 2017; Langevin et al. 2017) and MODFLOW-USG (Panday et al. 2013) and was tested using four example problems. Only the results from the MODFLOW 6 simulations are shown in this paper. In each example, accuracy of the simulation results obtained using the hydraulic-head formulation is assessed by comparison with independent results, such as simulation results from the well-established freshwater-head code SEAWAT (Langevin et al. 2008). In the third example, hydraulic-head formulation results are also compared against published results of a laboratory experiment. In the last example, hydraulic-head formulation results are also compared against published results from a pseudospectral approach and from the FEFLOW finite-element code.

The first example demonstrates numerical solution of the Henry seawater intrusion problem (Henry 1964).

The second example is a variation on the Henry problem (Simpson and Clement 2004) that features a dynamic seawater boundary and water-table fluctuations that span multiple model layers. This example demonstrates the use of the hydraulic-head formulation together with the Newton-Raphson formulation to solve this type of nonlinear problem, which is difficult to simulate with MODFLOW-based codes, such as SEAWAT, that use traditional cell-wetting and drying approaches. The third example uses the hydraulic-head formulation to simulate salinity patterns observed in the saltwater intrusion laboratory experiment of Goswami and Clement (2007). The fourth example is a natural convection Elder problem in which flow is driven purely by density differences.

Henry Problem

Variations on the Henry problem (Henry 1964) are commonly used as benchmark test problems for variable-density flow and transport codes. The model domain for the Henry problem is 2-m long by 1-m tall (Figure 1). In the original version of the problem, for which Henry (1964) presented a semianalytical solution, freshwater with a density of 1000 kg/m^3 flows into the domain through the left side at a rate of $5.702 \text{ m}^3/\text{d}$. Simpson and Clement (2004) reduced the rate of inflow to $2.851 \text{ m}^3/\text{d}$ in their numerical simulations, rendering the flow system less “advective dominant” and effecting “an increase in the relative importance of density-driven processes” (Simpson and Clement 2004). This modified version of the problem, called the “low-inflow” version here, provides a better benchmark test of density-dependent flow behavior than Henry’s original version. Results from both versions of the problem are presented.

Henry (1964) and Simpson and Clement (2004) assign the same flow and transport boundary conditions at the right boundary. The boundary condition for flow is a hydrostatic condition based on seawater concentration, 35 kg/m^3 , which corresponds to a density of 1024.5 kg/m^3 . For transport, the concentration at the right boundary is fixed at seawater concentration. The simulations presented here also include a variation in which the right boundary is assigned a mixed boundary condition: water that flows into the model from the right boundary enters at seawater concentration, and water that flows out of the model at the right boundary exits at the groundwater concentration computed for that boundary cell. Use of a mixed boundary condition in the Henry problem was introduced by Segol et al. (1975), who imposed a Neumann-type condition for transport when water flows out of the model. The mixed boundary condition used here, in which outflow is at the prevailing groundwater concentration, is the condition used for the Henry problem by Voss (1984) and Voss and Souza (1987). This manner of representing the seawater boundary, which is often used in saltwater intrusion models, allows a freshwater outflow zone to form above the zone of recirculating saltwater.

The freshwater hydraulic conductivity is set to 864 m/d , and the porosity to 0.35. Mechanical dispersion

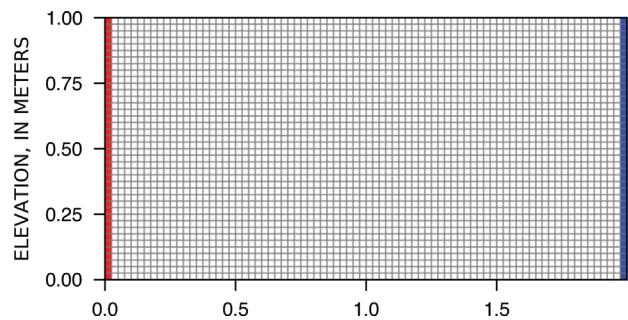


Figure 1. Model grid and boundary conditions used for the Henry problem. Freshwater inflow is specified for the cells shown in red on the left at a combined rate of $5.702 \text{ m}^3/\text{d}$ for the original problem and $2.851 \text{ m}^3/\text{d}$ for the low-inflow version of the problem. Cells shown in blue on the right side are specified as hydrostatic-seawater conditions.

is not represented; all mixing occurs solely by molecular diffusion with a diffusion coefficient of $1.62925 \text{ m}^2/\text{d}$. The simulation begins with the model domain initially filled with seawater, although the problem can also be simulated with the domain initially filled with freshwater. If the hydraulic head is fixed for the seawater boundary and the mixed boundary condition is used for transport, then it may be necessary to start the simulation with some saltwater in the domain or there may be no seawater inflow. In the simulations presented here, the domain is divided into 40 layers and 80 columns of cells, and a simulation period of 0.5 d is divided into 500 equally sized time steps of 0.001 d.

The original and low-inflow versions of the Henry problem were first simulated with concentration fixed at seawater along the right boundary (Figure 1). The hydrostatic (constant-head) and fixed-concentration boundary condition are imposed at the centers of cells along the right boundary. Figure 2 shows contours of fractional concentration relative to seawater concentration at the end of the 0.5 d simulation period. Visual comparison of contours for relative concentrations of 0.01, 0.1, 0.5, 0.9, and 0.99 shows very good agreement between results from the MODFLOW 6 hydraulic-head and the SEAWAT freshwater-head formulations.

The original and low-inflow versions of the Henry problem were then simulated with a mixed boundary condition for concentration in cells along the right boundary (Figure 3). The mixed boundary condition is represented using the general-head boundary (GHB) Package, which allows the hydrostatic boundary condition to be effectively imposed at the right edge of the model domain by accounting for the conductance of aquifer material between the cell center and the right edge of the model domain. Conceptually, a seawater reservoir is attached to the edge of each model cell at the right boundary. Flow into the model domain enters at the concentration of seawater, and flow out of the model domain exists at the concentration computed in the corresponding boundary cell. Figure 3 shows contours of

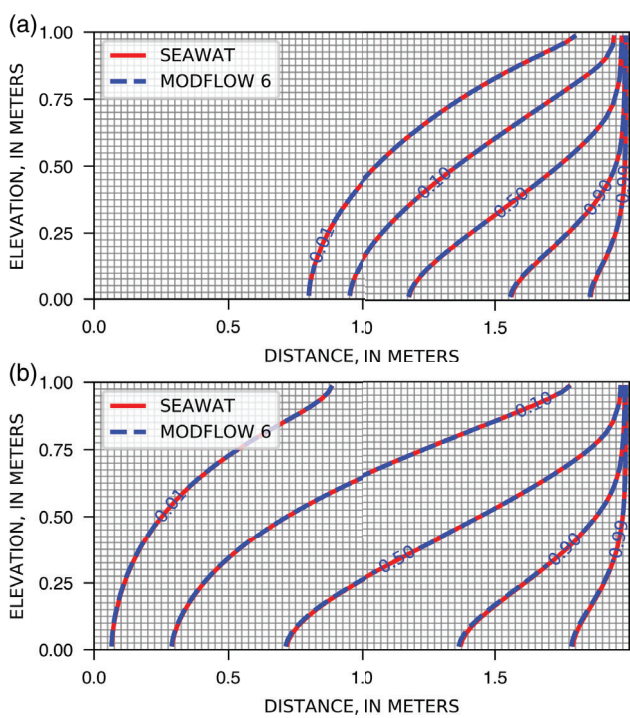


Figure 2. Simulation results for (a) the original Henry Problem and (b) the low-inflow Henry problem, in which the freshwater inflow rate is halved. For these simulations, the seawater boundary is treated as a specified-concentration boundary.

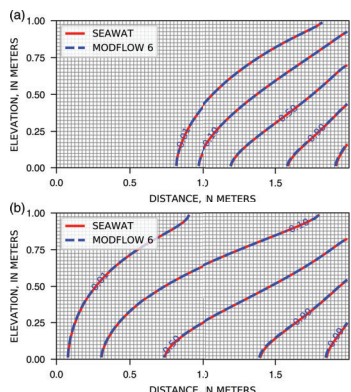


Figure 3. Simulation results for (a) the original Henry Problem and (b) the low-inflow Henry problem, in which the freshwater inflow rate is halved. For these simulations, the seawater boundary is treated as a mixed boundary condition in which inflow to the model from an external seawater reservoir enters at seawater concentration, but outflow from the model is assigned the concentration calculated in the corresponding boundary cell.

fractional concentration relative to seawater concentration at the end of the 0.5 d simulation period. As in the case of the fixed-concentration boundary condition, visual comparison of contours for relative concentrations of 0.01, 0.1, 0.5, 0.9, and 0.99 calculated using the mixed boundary condition shows very good agreement between results from the MODFLOW 6 hydraulic-head and the SEAWAT freshwater-head formulations.

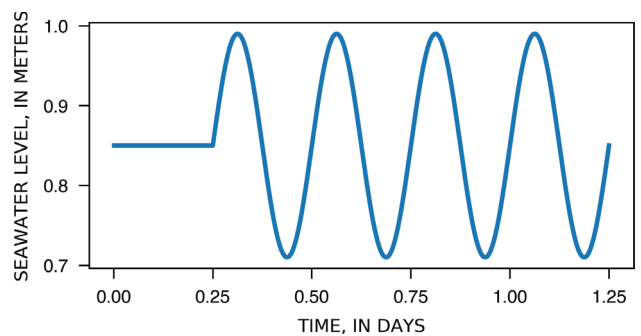


Figure 4. Sea level as a function of time for the Henry-type problem with a dynamic seawater boundary.

Fluctuating Seawater Boundary

The density-dependent, hydraulic-head formulation can be used with the Newton-Raphson formulation to simulate the rise and fall of the water table over multiple layers of model cells. The Henry problem described in the previous example is modified to include a fluctuating seawater boundary imposed on a sloped surface. This simulation represents groundwater flow processes that might be observed in a coastal aquifer affected by tidal fluctuations or longer-term changes in sea level. Approaches for representing these types of fluctuations with a variable-density groundwater model are described by Mulligan et al. (2011).

The total simulation period is 1.25 d. The first stress period, during which sea-level elevation remains constant at 0.85 m, is 0.25 d and is subdivided into time steps of 0.001 d. The remainder of the simulation consists of 1000 stress periods, each having a single time step of 0.001 d. During this 1-d period, sea level varies sinusoidally with time, with an amplitude of 0.14 m and a frequency of 4 per day, about an average value of 0.85 m, as shown in Figure 4. For the entire simulation period, a freshwater inflow rate of $1.425 \text{ m}^3/\text{d}$ is specified for the left boundary. This reduced freshwater inflow rate, which is approximately one-fourth the rate used for the original Henry problem, keeps the seawater from being completely flushed out of the domain.

The parameters for the simulation, including the size and shape of the model domain, are patterned after the Henry problem, except that the seawater boundary is applied to a sloped surface, as shown in Figure 5. Cells above the sloped surface (not shown) are inactive and do not participate in the simulation. Boundary conditions at cells along the sloped surface are assigned using an approach described by Mulligan et al. (2011) to simulate tidal boundary conditions with SEAWAT: cells inundated by seawater are assigned a GHB with the head set to sea level, and cells above sea level are assigned a drain condition with the elevation of the drain equal to the cell elevation. For the second part of the simulation, in which sea level varies according to Figure 4, the drains and general-head boundaries are reassigned on each stress period to account for changes in sea level. For example, as shown in Figure 5, with sea level at its average value

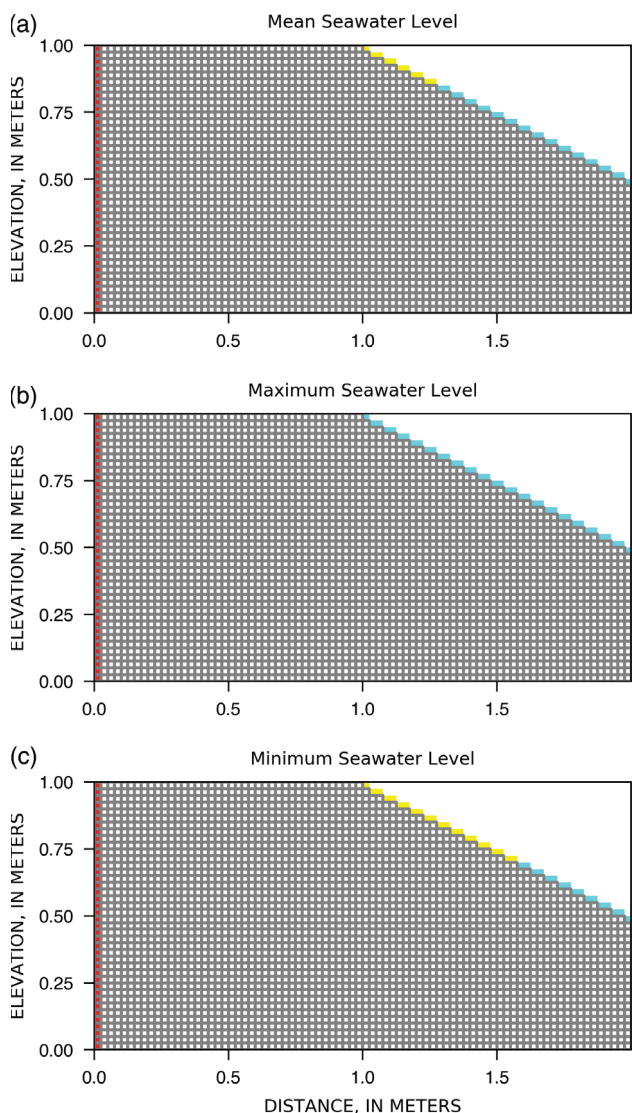


Figure 5. Model grid and boundary conditions used for the Henry-type problem with a dynamic seawater boundary, shown for the (a) average, (b) maximum, and (c) minimum sea levels. Freshwater inflow is specified for the cells shown in red on the left at a combined rate of $1.426 \text{ m}^3/\text{d}$. Cells shown in yellow on the right side are specified as drains with the drain elevation set to the cell elevation. Cells shown in cyan on the right side are specified as general-head boundaries with the head set from the fluctuating sea-level function in Figure 4.

of 0.85 m, the seven cells along the sloped surface that are above sea level are assigned drain conditions. The remaining cells along the sloped surface are below sea level and are assigned general-head boundaries. Figure 5 also shows the boundary configurations for the maximum and minimum sea levels.

Simulated results from the Henry-type problem with a dynamic sea level are shown in Figure 6 for three different times: (1) 0.25 d, the end of the first stress period, during which sea level was held constant at the mean value, (2) 0.312 d, the time of the first maximum sea level, and (3) 0.437 d, the time of the first minimum sea level. Cells shaded gray are considered dry in that

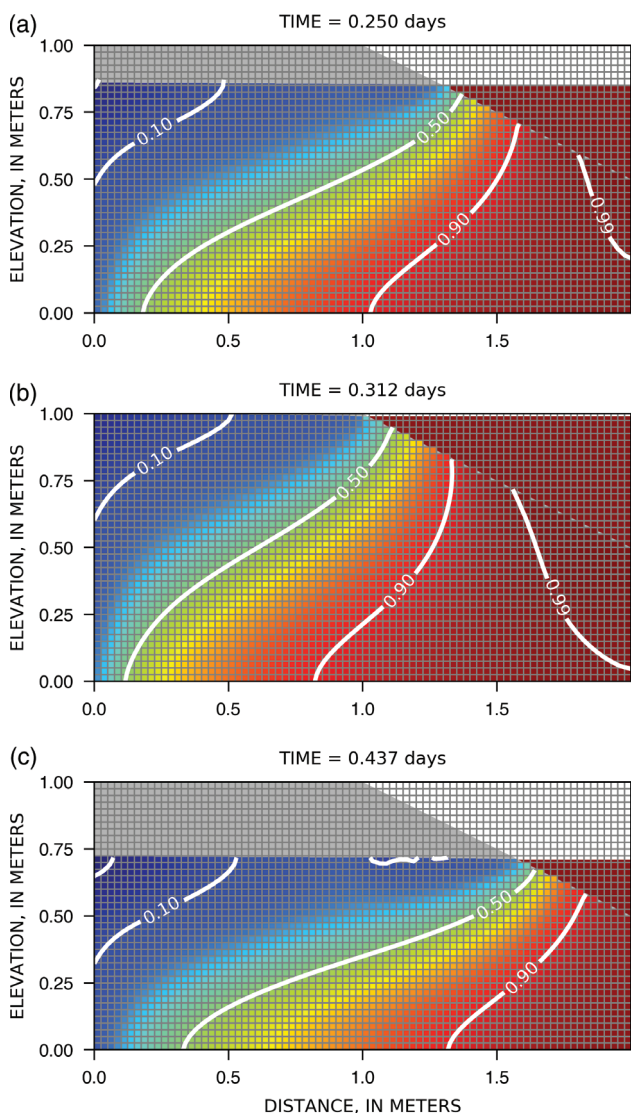


Figure 6. Simulated results for the Henry-type problem with a dynamic seawater boundary. Plots are for (a) the end of the first stress period, during which sea level is constant at 0.85 m, (b) the first maximum sea level, which occurs at 0.312 d, and (c) the first minimum sea level, which occurs at 0.437 d. Contours represent relative concentration (salinity) values and range from 0 (freshwater) to 1 (seawater).

their calculated hydraulic-head value is below the cell-bottom elevation; in this simulation, the head values of dry cells are equal to the water table elevation. Problems in which the water table rises and falls over multiple model layers can be difficult to simulate with groundwater codes (such as SEAWAT, for example) that are based on a traditional, MODFLOW-type cell-wetting and drying approach. The traditional wetting and drying approach can be highly unstable and often does not converge to a solution unless a Newton-Raphson formulation is used. This example demonstrates successful convergence, under conditions of repeated wetting and drying, of a numerical solution based on a combination of the density-dependent, hydraulic-head formulation and the Newton-Raphson formulation.

Saltwater Intrusion Laboratory Experiment

Goswami and Clement (2007) conducted an experimental study against which variable-density codes can be benchmarked. The experimental apparatus was a rectangular flow tank with internal dimensions of 53 cm (length) by 30.5 cm (height) by 2.7 cm (width). Formation and movement of saltwater wedges was induced by applying a constant-head saltwater boundary (density = 1.026 g/mL) on the left side of the tank and a constant-head freshwater boundary (density = 1.000 g/mL) on the right side of the tank. A schematic of the laboratory experiment, as represented in a corresponding SEAWAT model by Goswami and Clement (2007), is shown in Figure 7. To start the experiment, the system was allowed to equilibrate with a freshwater head of 26.7 cm applied to the right boundary. The corresponding steady-state condition is called SS-1. Next, the freshwater head at the right boundary was lowered to 26.2 cm, saltwater advanced into the tank from the left boundary, and movement of the interface between freshwater and saltwater was recorded. After about 80 min, the system effectively reached a new steady-state condition called SS-2. Last, the freshwater head at the right boundary was raised to 26.55 cm, which caused the interface between freshwater and saltwater to recede, and movement of the interface was recorded until a final steady-state condition, called SS-3, was effectively reached. Measurements of the interface position during advance and recession and at the three steady-state positions, as well as freshwater inflow rates for the three steady-state conditions, are reported in Goswami and Clement (2007). Simulations of the experiment by Goswami and Clement (2007) using SEAWAT showed that the code is capable of simulating the observed saltwater-intrusion dynamics.

A MODFLOW 6 model with the hydraulic-head formulation was developed to simulate the saltwater-intrusion experiment of Goswami and Clement (2007). The model is constructed using a grid of 0.5-cm square cells. The saltwater (left) and freshwater (right) boundaries are represented using general-head boundaries

that provide hydraulic resistance equivalent to a half-cell of aquifer material, thereby effectively moving the specified heads to the outer edges of the model domain. (In the SEAWAT model of Goswami and Clement 2007, constant-head boundaries were applied to the centers of the boundary cells, which are located one-half cell width in from the outer edges of the model domain.) At the freshwater (right) boundary, a different head value is assigned to each stress period. Assignment of the remaining parameter values, including a hydraulic conductivity of 1050 m/d and a porosity of 0.385, is consistent with the experimental setup and SEAWAT model of Goswami and Clement (2007). Three stress periods are used to represent (1) equilibration to the SS-1 position, (2) advance of the interface to SS-2, and (3) recession of the interface to SS-3. The three stress periods are 60, 80, and 60 min long, respectively, with 1-s time steps. The flow equation is solved for each time step with a steady-state approximation by neglecting water storage changes. The transport equation is solved for transient conditions to represent movement of the interface.

Figure 8 shows the width of the transition zone between freshwater and saltwater for the SS-2 condition, simulated using MODFLOW 6 with the hydraulic-head formulation. Concentration is expressed as concentration (salinity) relative to the saltwater-inflow concentration. The width of the transition zone for the MODFLOW 6 simulation is as large as about 5 cm, whereas the width for the SEAWAT simulation of Goswami and Clement (2007) is about 1 cm. The observed interface between freshwater and saltwater is narrow and difficult to represent accurately with a dispersive solute transport model. With the model grids used for the simulations discussed here, the amount of mixing that occurs in the laboratory experiment is less than the numerical dispersion. Therefore, in both the MODFLOW 6 simulations presented here and the SEAWAT simulations presented by Goswami and Clement (2007), molecular diffusion and hydrodynamic dispersion were not represented explicitly in the models. Compared to SEAWAT, results from MODFLOW 6 exhibit greater numerical dispersion. This is primarily

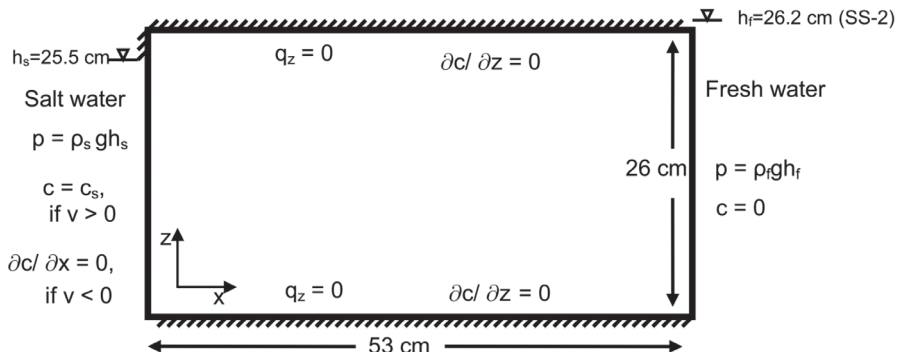


Figure 7. Diagram showing the configuration of the saltwater intrusion laboratory experiment and corresponding SEAWAT model by Goswami and Clement (2007). Reproduced with permission from Figure 4 of Goswami and Clement (2007).

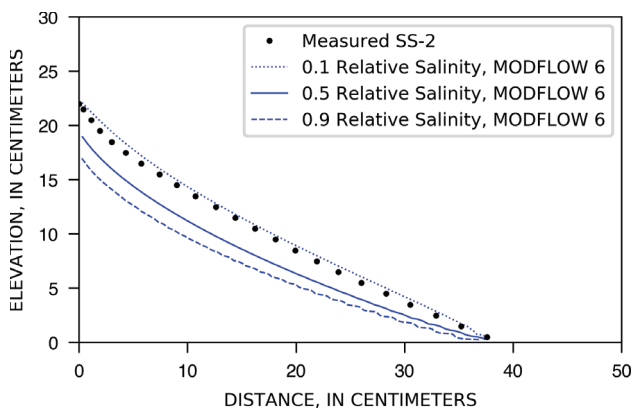


Figure 8. Comparison of simulated 0.1, 0.5, and 0.9 relative-salinity contours with experimental measurements of saltwater-freshwater interface position by Goswami and Clement (2007) at steady state SS-2. Modified from Figure 6 of Goswami and Clement (2007) to show MODFLOW 6 results.

because the explicit third-order TVD scheme in MT3DMS (Zheng and Wang 1999), upon which SEAWAT is based, is better at maintaining sharp concentration fronts, such as those observed in the laboratory experiment, than the implicit second-order TVD scheme implemented in MODFLOW 6.

For benchmarking of the SEAWAT code, Goswami and Clement (2007) compared the 0.5 relative-salinity contour with measured interface positions, although, because of the narrow simulated transition zone, selection of the 0.1 or 0.9 relative-salinity contour instead would have yielded similar results. In the MODFLOW 6 examples shown here, in which the simulated transition zone is wider than in the SEAWAT simulations, the 0.2 relative-salinity contour provides a better approximation of the measured interface position and movement than the 0.5 relative-salinity contour. MODFLOW 6 simulations with finer grids (results not shown) resulted in less numerical dispersion, narrower transition zones, and further advance of the 0.5 relative-salinity contour toward the measured interface positions.

Figure 9 compares the simulated interface position, as represented by the 0.2 relative-salinity contour, with experimental data for the three steady-state conditions. Results for advancing and receding saltwater interface positions are presented in Figures 10 and 11, respectively. For SS-1, the measured and simulated freshwater inflow rates are 1.42 and 1.41 cm³/s, respectively. For SS-2, the measured and simulated freshwater inflow rates are 0.59 and 0.60 cm³/s, respectively. For SS-3, the measured and simulated freshwater inflow rates are 1.19 and 1.17 cm³/s, respectively. Simulated interface positions and freshwater inflow rates simulated using MODFLOW 6 with the hydraulic-head formulation generally compare well with the experimental data of Goswami and Clement (2007), showing the ability of the code to represent saltwater-intrusion dynamics.

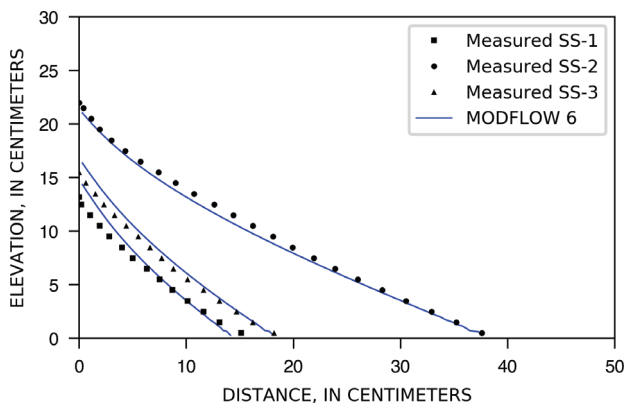


Figure 9. Comparison of simulated saltwater to freshwater interface positions, represented by 0.2 relative-salinity contours, with experimental measurements of interface position by Goswami and Clement (2007) at steady states SS-1, SS-2, and SS-3. Modified from Figure 5 of Goswami and Clement (2007) to show MODFLOW 6 results.

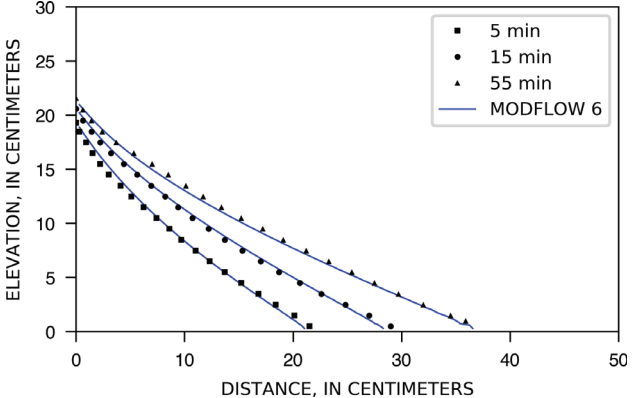


Figure 10. Comparison of simulated saltwater to freshwater interface positions, represented by 0.2 relative-salinity contours, with experimental measurements of interface position by Goswami and Clement (2007) at three times (5, 15, and 55 min) at which the interface was advancing. Modified from Figure 7 of Goswami and Clement (2007) to show MODFLOW 6 results.

Natural Convection Elder Problem

A common test for coupled variable-density flow and transport models is the classic Elder problem (Elder 1967), in which fluid flow is driven purely by density differences. In the original Elder problem, natural convection is driven by density differences arising from temperature variations. The original Elder problem was modified by Voss and Souza (1987) into a solute-transport analog in which density variations result from spatial variations in solute concentration. In the solute-transport analog, sinking salt plumes drive natural convection. A complication with the use of the Elder problem for testing purposes is the existence of multiple stable and unstable solutions (Johannsen 2003), which led van Reeuwijk et al. (2009) to explore variations on the Elder problem that have only one solution. van Reeuwijk et al. (2009) designed a variation on the Elder solute-transport problem by reducing the

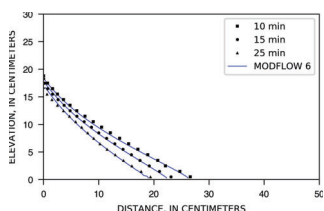


Figure 11. Comparison of simulated saltwater to freshwater interface positions, represented by 0.2 relative-salinity contours, with experimental measurements of interface position by Goswami and Clement (2007) at three times (10, 15, and 25 min) at which the interface was receding. Modified from Figure 8 of Goswami and Clement (2007) to show MODFLOW 6 results.

density contrast and lowering the Rayleigh number from the value of 400 used in the classic version to a value of 60. van Reeuwijk et al. (2009) solved the Elder problem using a pseudospectral approach that was free of the numerical dispersion that is common with finite volume and finite element solutions. They ensured the reliability of the pseudospectral approach by comparing results with an analytical solution and also with results from FEFLOW simulations. According to van Reeuwijk et al. (2009), this low Rayleigh number variation on the Elder problem is better suited for benchmarking than the classic version because only one solution exists at the lower Rayleigh number.^{9,5} In the test problem described in this section, the hydraulic-head formulation, as implemented in MODFLOW 6, is used to simulate the low Rayleigh number Elder problem proposed by van Reeuwijk et al. (2009). Also included in this section is a MODFLOW 6 simulation of the high Rayleigh number Elder problem to show the performance of the hydraulic-head formulation for much larger density contrasts.

A schematic diagram for the Elder problem described by van Reeuwijk et al. (2009) is shown in Figure 12. The problem consists of a two-dimensional cross-sectional domain that is surrounded on all sides by impermeable boundaries. Along the bottom edge, the concentration is fixed at a value of c_0 . The concentration is fixed at a value of c_0 along the top and bottom edges of the domain, except within a section in the middle of the top edge where the concentration is fixed at a higher value of c_1 . The parameter values used for the simulations are based on values reported by Voss and Souza (1987) and by Guo and Langevin (2002) for benchmarking of the SEAWAT program with the Elder problem. The height of the box (H) was set to 150 m. The reference hydraulic conductivity K_0 , which is the hydraulic conductivity of a medium saturated with freshwater, was specified as 0.411 m/d. The diffusion coefficient D_m was specified as 0.308 m²/d. A value of 0.1 was assigned for porosity (θ). The dependence of density on concentration was represented using the linear relation $\rho = \rho_0 + E(c' - c_0)$, where E is given a value of 0.7. With these values, and a value of zero assigned for c_0 , different Rayleigh numbers were tested by adjusting the maximum solute concentration c_1 . With the variable definitions used in this

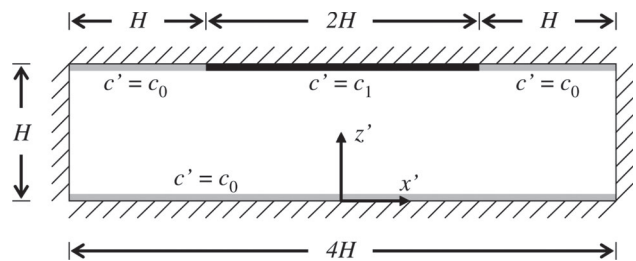


Figure 12. Diagram showing the configuration of the Elder problem. Reproduced with permission from Figure 1 of van Reeuwijk et al. (2009).

paper, the Rayleigh number (Ra) equation is:

$$Ra = \frac{EK_0(c_1 - c_0)H}{\rho_0 \theta D_m} \quad (27)$$

For a low Ra of 60, the value for c_1 is calculated to be 42.86 kg/m³, which gives a density difference of 31.5 kg/m³ between c_1 and c_0 . For the high Ra of 400, the value for c_1 is 285.71 kg/m³, which gives a density difference of 200 kg/m³ between c_1 and c_0 .

The hydraulic-head formulation implemented in MODFLOW 6 and the equivalent freshwater head formulation implemented in SEAWAT were used to simulate the low Ra Elder problem with a grid consisting of 52 layers and 88 columns. van Reeuwijk et al. (2009) restricted their pseudospectral calculations to one-half of the domain under an assumption of symmetry, whereas the simulations here encompass the entire 600 m by 150 m domain. The 50 middle layers have 3-m layer thicknesses; thicknesses for the top and bottom layers were set to be 1/10 this thickness to more precisely represent the location of the specified concentration boundaries and honor the problem domain height of 150 m. The hydraulic conductivity value for these top and bottom layers was set to a small value (1×10^{-8} m/d) to eliminate advective flow through these cells. In the horizontal direction, cells were assigned uniform spacings of 6.818 m. The total simulation time was set to 73,000 d, which was divided into 10,000 equally sized 7.3-d time steps. Testing with the various solution schemes indicated that the central-in-space advective scheme resulted in the least amount of numerical dispersion, so the simulations reported here all use central-in-space weighting.

Results from simulations are shown in Figure 13. The left panel of Figure 13 shows a comparison between MODFLOW 6 and SEAWAT for the entire model domain for four different times (6, 20, 60, and 200 years). The hydraulic-head formulation shows excellent agreement with the proven equivalent freshwater head formulation in SEAWAT. The right panel of Figure 13 shows a comparison between the MODFLOW 6 hydraulic-head formulation results and the pseudospectral results and FEFLOW results reported by van Reeuwijk et al. (2009). As with the SEAWAT comparison, the hydraulic-head formulation shows excellent agreement with other simulation approaches.

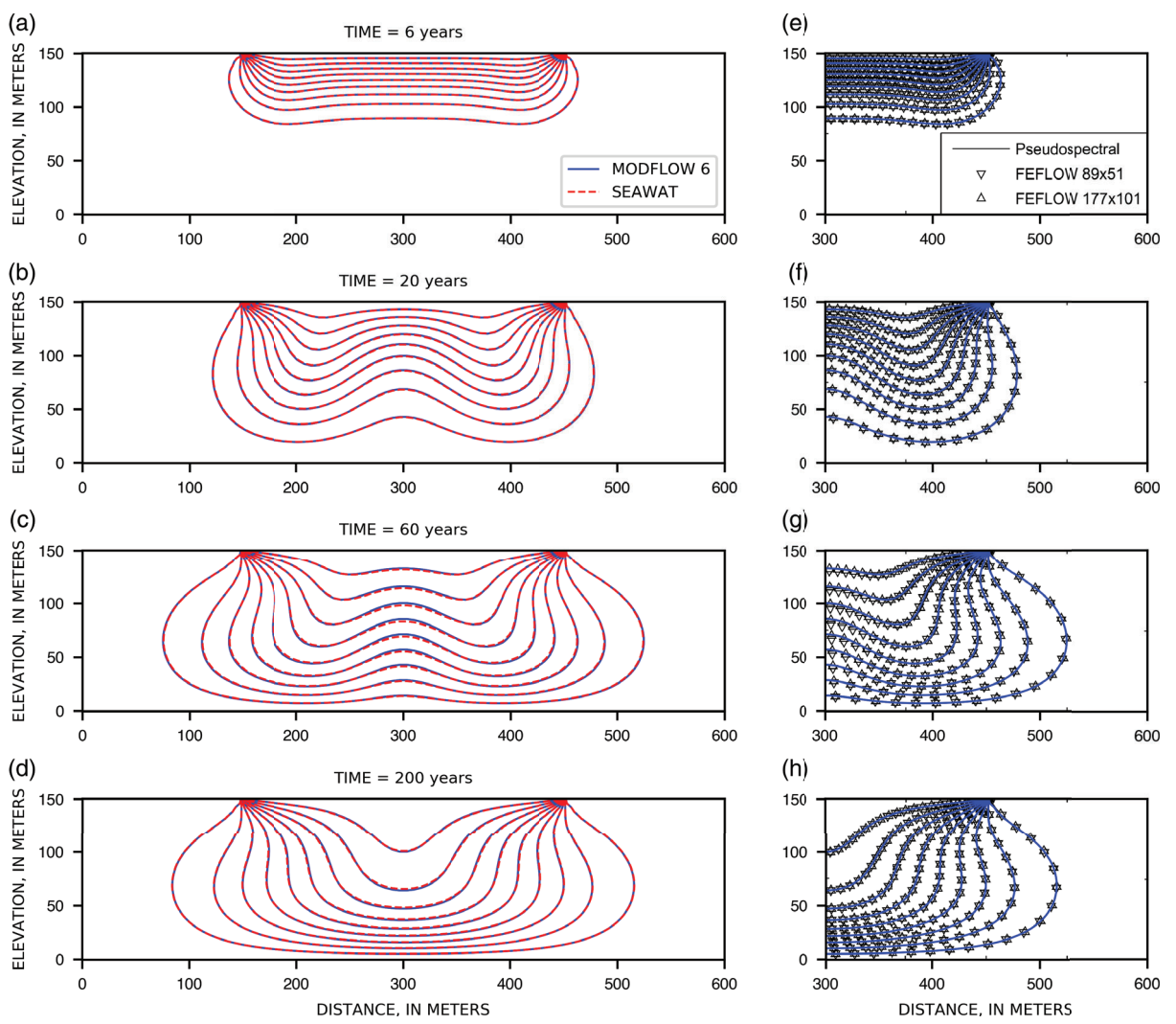


Figure 13. Comparison of simulated salinity contours for the low Ra Elder problem. Comparison is between MODFLOW 6 and (a-d) full-domain SEAWAT simulations and (e-h) half-domain results for the pseudospectral approach and FEFLOW simulations with two different grid resolutions, from van Reeuwijk et al. (2009). Contours represent relative concentration values and range from 0.1 to 0.9 with a contour interval of 0.1.

To evaluate the accuracy of the hydraulic-head formulation for a larger density contrast, the high Rayleigh number Elder problem ($Ra = 400$) was also simulated with MODFLOW 6. As mentioned earlier, there are multiple valid solutions for the high Ra Elder problem; van Reeuwijk et al. (2009) presented pseudospectral results for three, stable steady-state configurations. Steady-state results from the MODFLOW 6 simulation clearly correspond to one of the three stable solutions reported by van Reeuwijk et al. (2009). A comparison between this stable solution and the MODFLOW 6 results is shown in Figure 14. As determined by Johannsen (2003), steady-state solutions for the Elder problem are not sensitive to whether or not a mass-based or volume-based conservation equation is used for flow; however, the MODFLOW 6 results show excellent agreement with the pseudospectral approach, even for a problem that involves a very large density contrast. Additional work is needed to determine the limitations of the volume-based conservation equation

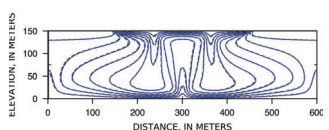


Figure 14. Comparison of simulated salinity contours for the high Ra Elder problem between MODFLOW 6 (blue) and the pseudospectral approach (black) reported by van Reeuwijk et al. (2009). Results are for a stable configuration after a simulation period of 200 years. Contours represent relative concentration values and range from 0.1 to 0.9 with a contour interval of 0.1.

for simulating practical problems with large density variations.

Summary and Conclusions

Variable-density groundwater modeling programs have traditionally used freshwater head as the dependent

variable. There are a number of advantages to solving variable-density groundwater flow using freshwater head. The freshwater-head formulation is easy to conceptualize, and for horizontal flow, the freshwater-head gradient is the sole driving force. Moreover, the generalized form of Darcy's Law consists of a distinct freshwater-head term and a separate density-dependent term, which makes it convenient to use for flux calculations. There are a number of disadvantages for using the freshwater-head formulation, however, including the difficulty of implementing it in an existing groundwater modeling program that is based on a constant-density formulation. For shallow aquifer simulations, the freshwater-head formulation typically requires repeated conversion between freshwater head and hydraulic head within the modeling code to determine whether cells are confined, unconfined, or dry. The freshwater-head formulation can also make other calculations more complex, such as calculation of Jacobian derivative terms for the Newton-Raphson method or expansion to account for turbulent flow.

This paper presents a hydraulic-head formulation for variable-density groundwater flow. The generalized form of Darcy's Law is written in terms of hydraulic head and is compared with an analogous equation written in terms of freshwater head. An approach is proposed for extending constant-density groundwater modeling codes to include variable-density effects as correction terms that are added to the system of equations resulting from application of the control-volume finite-difference method to constant-density flow. To demonstrate the hydraulic-head formulation, the correction terms were implemented in the MODFLOW 6 and MODFLOW-USG programs, and four example problems were simulated with the new formulation. Results of the MODFLOW 6 simulations are presented in this paper. In the first two examples, the hydraulic-head formulation was shown to give nearly identical results to the well-established SEAWAT code for several different variations of the Henry problem. The second example problem was specifically designed to show the benefits of the hydraulic-head formulation in simulating the rise and fall of the water table over multiple model layers in response to sinusoidally varying boundary condition. Simulation of problems in which the water table crosses model layers is difficult with a saturated variable-density groundwater modeling code such as SEAWAT, but was shown here to be possible with a combination of the hydraulic-head formulation with the Newton-Raphson method. In the third example, the hydraulic-head formulation was shown to be capable of simulating a laboratory experiment (Goswami and Clement 2007) that featured advancing and receding saltwater intrusion. The last example demonstrates application of the hydraulic-head formulation to a problem of natural convection in which fluid flow is driven purely by density differences. Based on these successful benchmark examples and the mathematical derivations presented here, the hydraulic-head formulation is shown to be analogous to the equivalent freshwater head formulation and other formulations used for variable-density groundwater flow. The hydraulic-head

formulation offers an advantage in that it can be implemented in a constant-density program without having to make changes wherever hydraulic head and saturated thicknesses are needed.

Acknowledgments

The authors thank Rohit Goswami for suggesting the advancing and receding saltwater interface problem as a way to demonstrate the hydraulic-head formulation. The authors also thank Vivek Bedekar, Vincent Post, and an anonymous reviewer for constructive comments that substantially improved the paper.

Supporting Information

Additional supporting information may be found online in the Supporting Information section at the end of the article. Supporting Information is generally *not* peer reviewed.

Appendix S1: Supporting information

References

- Danish Hydrologic Institute. 1998. *Mike she water movement—User guide and technical reference manual, edition 1.1*. Technical report, Danish Hydrologic Institute, Horsholm, Denmark.
- Elder, J.W. 1967. Transient convection in a porous medium. *Journal of Fluid Mechanics* 27, no. 3: 609–623.
- Goswami, R.R., and P. Clement. 2007. Laboratory-scale investigation of saltwater intrusion dynamics. *Water Resources Research* 43, no. W04418.
- Guo, W., and C.D. Langevin. 2002. *User's guide to SEAWAT: A computer program for simulation of three-dimensional variable-density ground-water flow*. U.S. Geological Survey Techniques of Water-Resources Investigations Book 6, chap. A7, 77. Reston, Virginia: USGS.
- Harbaugh, A.W., Banta, E.R., Hill, M.C., and McDonald, M.G. 2000. User guide to modularization concepts and the ground-water flow process, MODFLOW-2000 the U.S. Geological Survey modular ground-water model. U.S. Geological Survey Open-File Report 00-92, 121 p. Reston, Virginia: USGS.
- Harbaugh, A.W. 2005. *MODFLOW-2005, the U.S. Geological Survey modular ground-water model—the Ground-Water Flow Process*. In *U.S. Geological Survey Techniques and Methods, Book 6* chap. A16. Reston, Virginia: USGS.
- Henry, H. 1964. Effects of dispersion on salt encroachment in coastal aquifers. *Sea Water in Coastal Aquifers*, U.S. Geological Survey Supply Paper, 1613-C, C71-C84.
- Hughes, J.D., C.D. Langevin, and E.R. Banta. 2017. Documentation for the MODFLOW 6 framework. U.S. Geological Survey Techniques and Methods, Book 6 chap. A57, 36 p.p.
- Johannsen, K. 2003. On the validity of the Boussinesq approximation for the elder problem. *Computational Geosciences* 7, no. 3: 169–182.
- Langevin, C.D., J.D. Hughes, A.M. Provost, E.R. Banta, R.G. Niswonger, and S. Panday. 2017. *Documentation for the MODFLOW 6 groundwater flow (GWF) model*. U.S. Geological Survey Techniques and Methods, Book 6 chap. A55, 197 p. Reston, Virginia: USGS.
- Langevin, C.D., D.T. Thorne Jr, A.M. Dausman, M.C. Sukop, and W. Guo. 2008. SEAWAT version 4—A computer

- program for simulation of multi-species solute and heat transport. U.S. Geological Survey Techniques and Methods, book 6 chap. A22, 39 p.
- Langevin, C.D., Shoemaker, W.B., and Guo, W. 2003. MODFLOW-2000 the U.S. Geological Survey modular ground-water model—documentation of the SEAWAT-2000 version with the variable-density flow process (VDF) and the integrated MT3DMS transport process (IMT). U.S. Geological Survey Open-File Report 03-426, 43 p. Reston, Virginia: USGS.
- de Marsily, G. 1986. *Quantitative Hydrogeology*. New York, New York: Academic Press, Inc.
- McDonald, M.G., and A.W. Harbaugh. 1988. A modular three-dimensional finite-difference ground-water flow model. U.S. Geological Survey Techniques of Water-Resources Investigations, Book 6 chap. A1, 586 p.
- Mulligan, A., C.D. Langevin, and V.E.A. Post. 2011. Tidal boundary conditions in SEAWAT. *Groundwater* 46, no. 6: 866–879.
- Niswonger, R.G., S. Panday, and M. Ibaraki. 2011. MODFLOW-NWT, a Newton formulation for MODFLOW-2005. U.S. Geological Survey Techniques and Methods, Book 6 chap. A37, 44 p.
- Oude Essink, G.H.P. 1998. MOC3D adapted to simulate 3D density-dependent groundwater flow. In *Proceedings of the MODFLOW'98 Conference*, October 4–8, 1998, Golden, Colorado, USA, volume 1, 291–303.
- Panday, S., C.D. Langevin, R.G. Niswonger, M. Ibaraki, and J.D. Hughes. 2013. MODFLOW-USG version 1—An unstructured grid version of MODFLOW for simulating groundwater flow and tightly coupled processes using a control volume finite-difference formulation. U.S. Geological Survey Techniques and Methods, Book 6 chap. A45, 66 p.
- van Reeuwijk, M., S.A. Mathias, C.T. Simmons, and J.D. Ward. 2009. *Water Resources Research* 45, W04416, doi:10.1029/2008WR007421.
- Segol, G., G.F. Pinder, and W.G. Gray. 1975. A Galerkin-finite element technique for calculating the transient position of the saltwater front. *Water Resources Research* 11, no. 2: 343–347.
- Shoemaker, W.B., E.L. Kuniansky, S. Birk, S. Bauer, and E.D. Swain. 2008. Documentation of a conduit flow process (CFP) for MODFLOW-2005. U.S. Geological Survey Techniques and Methods, Book 6 chap. A24, 50 p. Reston, Virginia: USGS.
- Simpson, M.J., and T.P. Clement. 2004. Improving the worthiness of the Henry problem as a benchmark for density-dependent groundwater flow models. *Water Resources Research* 40, no. W01504: 1152–1173.
- Simunek, J., Šejna, M., and Van Genuchten, M. 1998. The HYDRUS-2D software package for simulating water flow and solute transport in two dimensional variably saturated media, version 2.0.
- Voss, C.I., and W.R. Souza. 1987. Variable density flow and solute transport simulation of regional aquifers containing a narrow freshwater-saltwater transition zone. *Water Resources Research* 23, no. 10: 1851–1866.
- Voss, C.I. 1984. SUTRA—A finite-element simulation model for saturated-unsaturated fluid-density-dependent groundwater flow with energy transport or chemically-reactive single-species solute transport. U.S. Geological Survey Water-Resources Investigations Report 84-4369, 409 p. Reston, Virginia: USGS.
- Zheng, C. and Wang, P. P. (1999). MT3DMS—A modular three-dimensional multi-species transport model for simulation of advection, dispersion and chemical reactions of contaminants in groundwater systems; Documentation and user's guide. Contract report SERDP-99-1: Vicksburg, Mississippi: U.S. Army Engineer Research and Development Center, 169 p.



GROUNDWATER FOUNDATION
Protect. Connect. Inspire.

You make a difference.
Text **GROUNDWATER25** to **20222** to make a one-time **\$25** donation to the Groundwater Foundation.



A one-time donation of \$25.00 will be added to your mobile phone bill or deducted from your prepaid balance. All charges are handled by a third party mobile service provider. User must be age 18 or older and parent/guardian to participate. By sending YES, the user agrees to the terms and conditions. Service is available on most carriers. Message & Data Rates May Apply. Donations are collected for the benefit of the Groundwater Foundation by the Mobile Giving Foundation and subject to the terms found at www.hmgf.org/. You can unsubscribe at any time by texting STOP to short code "20222" text HELP to "20222" for help.

PROTECT.
Groundwater is vital to our life and livelihood, and understanding groundwater is the first step to protecting it from today and tomorrow.

CONNECT.
We connect businesses, and communities through local groundwater education and action making us all part of the solution for clean sustainable groundwater.

INSPIRE.
Every person plays a role in protecting and conserving groundwater.

Learn more: groundwater.org